Int. J. Dev. Biol. 50: 405-412 (2006)
doi: 10.1387/ijdb.052007st

Original Article

The dynamic nature of mollusc egg surface architecture and its relation to the microtubule network

SHEENA E.B. TYLER* and SUSAN J. KIMBER

Faculty of Life Sciences, University of Manchester, England

ABSTRACT Dynamic changes in the surface architecture pattern of embryos of the slipper limpet (*Crepidula fornicata, Mollusca*) were found in this study to correlate with the dynamic activity and pattern of the underlying mitotic spindle microtubule network, revealed by fluorescent labelling and confocal imaging techniques. Examination of a series of optical sections indicate that this network appears to be spatially co-ordinated together as a whole throughout the embryo. The microtubule pattern also associated with abnormal multipolar spindles resulting from an applied static magnetic field, indicating that the pattern may be generated by a natural endogenous field source. The patterning characteristics of the surface and microtubule network together provide further morphological evidence for a primary morphogenetic or developmental field system which organises the primary body axis and co-ordinates the pattern of cleavage.

KEY WORDS: *architecture, magnetic field, microtubule, morphogenetic, spindle*

Introduction

A visible marker of a morphogenetic field may be provided by the surface architecture on cleaving eggs of the marine gastropod mollusc, *Crepidula fornicata* (Tyler *et al*., 1998). The morphogenetic field (Dreisch,1891), has been described as a spatial domain in which each part has a state determined by the state of neighbouring parts, so that the whole has a specific relational structure. (Goodwin, 1984, 1985). Moreover, mechano-chemical fields based on cytoskeletal–ionic interactions may provide a generative basis of morphogenesis (Goodwin and Trainor, 1985), which remains so elusive.

We provided three lines of evidence from our observations linking the molluscan surface architecture to a putative field system. Firstly, the architecture, consisting of linear arrays of ridges (first observed vegetally by Dohmen and van der Mey, 1977), is organised with reference to the animal-vegetal (a-v) axis, which in turn is spatially related to the anterior-posterior (a-p) axis of the subsequent embryo and larvae. Secondly, in mollusc eggs, successive cleavage quartets are produced by a spiral cleavage mode around the a-v axis. The surface architecture is also orientated with reference to these specific micromere quartets. Thus the surface architecture may be a morphological marker for a field system which organises the a-v axis and the cleavage pattern. Thirdly, the animal-vegetal architecture organisation correlates with the animal-vegetal polarity of ionic current pattern in eggs of the mollusc, *Lymnaea* (Zivkovic *et al*., 1990, Creton *et al.*, 1993). Such ionic current patterns reflect a polarised endogenous DC current driven through embryos (Shi and Borgens, 1995). This phenomenon is widespread throughout animal and plant taxa, foreshadowing certain developmental events for which they may thus have a causal role.

The surface architecture ridges are revealed by FITC-conjugated lectins, probably because the ridges provide an increased surface area which can accommodate more lectin-binding receptors (Dohmen, 1992). The ridges can also be delineated by cryo-SEM (Tyler *et al*., 1998).

One of the clearest examples of a direct role for ionic currents in morphogenesis is in the polarising fucoid egg, in which an intracellular Ca^{2+} flux orientates rhizoid growth (Nuccitelli 1978, 1988; Jaffe *et al*., 1987). Another example is the insect ovarian follicle, in which an intracellular voltage gradient generates the polarity of protein transport, influencing oocyte polarity (Woodruff and Telfer, 1973, 1980). Ion currents are also involved in early cleavage, for instance polar lobe formation in mollusc eggs (Zivkovic and Dohmen, 1991) and

Abbreviations used in this paper: a-p, anterior-posterior; a-v, animal-vegetal; CR, centre of radius; GSL, Griffonia simplicifolia lectin.

***Address correspondence to:** Dr. Sheena E.B. Tyler. Faculty of Life Sciences, University of Manchester, Stopford Building, Oxford Rd., Manchester, M13 9PT, England. Fax: +44-161-295-3938. e-mail: sheena.tyler@man.ac.uk

Electronic Supplementary Material for this paper is available following the "Supplementary Material" link at: http://www.intjdevbiol.com/web/paper.php?doi=052007st

0214-6282/2006/$25.00

Printed in Spain
www.intjdevbiol.com

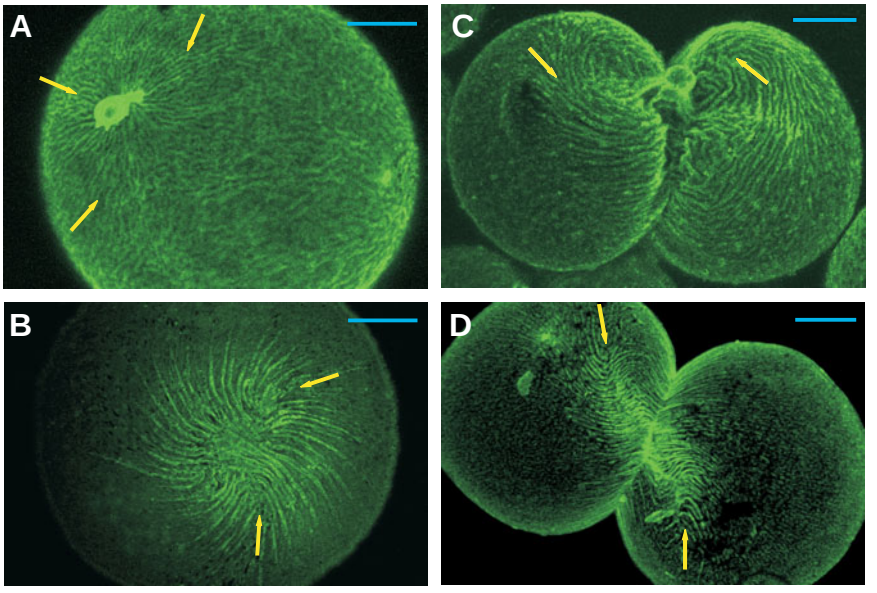

Fig. 1. Surface architecture features of uncleaved eggs and 2-cell stages revealed by FITC-GSL-1 lectin staining. (A) *The animal surface of an uncleaved egg, with no organisation of pattern evident, except for ridges radiating (arrowed) from the animal pole region.* **(B)** *The ventral region of an uncleaved egg, with surface architecture ridges swirling (arrowed) from the vegetal pole region.* **(C,D)** *Swirls of surface architecture (arrowed) during 4-cell formation on the animal surface (C) and vegetal surface (D). Scale bar, 50 μm.*

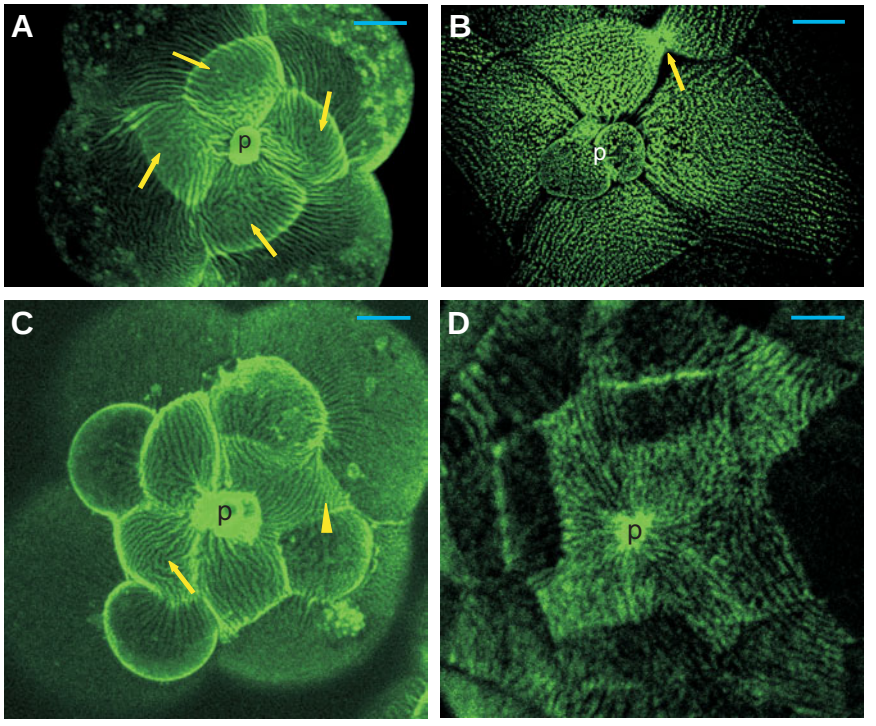

Fig. 2. Development of surface architecture pattern from 8-cell to later cleavage stages, as revealed by FITC - GSL-1 lectin-staining. (A) *8-cell formation. Ridges of architecture (arrowed) swirl over the region of 1st micromere quartet formation.* **(B)** *13-cell stage of 16-cell formation. The arrow indicates dextral swirl of surface architecture, whereas the arrowhead denotes architecture swirling into a developing $1q^2$ cell.* **(C)** *16-cell formation. The surface architecture pattern is constricted (arrow) between $1q^1$ and $1q^2$ cells.* **(D)** *Later cleavage stage, showing surface architecture continuity between cells as it radiates out from animal pole region. p, polar body, denoting animal pole. Scale bars: A,B, 50 μm; C,D, 25 μm.*

mouse blastomere polarisation (Nuccitelli and Wiley, 1985). An outward flow of ionic current pattern predicts limb bud location and development (Borgens *et al.*, 1983; Robinson, 1983) and has been implicated in limb regeneration (Borgens *et al.*, 1977, 1984; Eltinge *et al.*, 1986), wound regeneration (Stump and Robinson, 1983; Jaffe and Vanable, 1985; Chiang *et al.*, 1991; Nuccitelli, 2003) and spinal cord neuronal regeneration (Borgens *et al.*, 1987, 1990, 1999); amphibian neural tube formation (Metcalf *et al.*, 1994); neural crest cell migration (Cooper and Keller, 1984); neurite projection (Hinkle *et al.,* 1981; McCaig, 1987; Borgens and McCaig, 1989); lens development (Parmalee *et al.*, 1985); and chick tail morphogenesis (Hotary and Robinson, 1990).

A more precise role of ionic currents in development has been elucidated by applied magnetic fields leading to perturbations of development. In frog eggs, for example, the cleavage furrows align in parallel with the magnetic field vector (Denegre *et al.*, 1998). Embryogenesis is also affected in the chick (Ubada *et al.*, 1985; Jutilainen *et al.*, 1986; Koch *et al.*, 1993), *Drosophila* (Ho *et al.*, 1992) and the sea urchin (Levin and Ernst, 1997).

In this study, firstly we explore the tempero-spatial characteristics of the surface architecture during cleavage of *Crepidula* embryos, asking the question: is the architecture static once formed, or does it develop in complexity? Secondly we explore the tempero-spatial characteristics of the underlying microtubule network: what is the relationship between the surface and the microtubules, if any? Thirdly we apply magnetic fields within the physiological range to cleaving *Crepidula* eggs. The rationale for this is that if the architecture is generated by a transembryonic electromagnetic field, then perturbation of that field is likely to result in visible effects upon the architecture.

Results

Surface architecture

FITC-conjugated GSL-1 lectin labelled embryos revealed the following characteristics.

Uncleaved eggs to 4-cell stage

Ridges of surface architecture radiated out from the animal pole, but elsewhere on the animal surface no pattern was evident (Fig. 1A). A more prominent surface architecture radiated out from the vegetal pole (Fig. 1B). During first cleavage, the ridges radiating from the animal pole lengthened. Later, during second cleavage, swirls of ridges were observed on the animal and vegetal surface (Figs. 1C

and D). At this stage, the leading edge of the swirl on one blastomere was orientated in the opposite direction to that of the neighbouring blastomere. Distinct regions of architecture pattern were noted, in which the ridges radiated out from a central point (centre of radius [CR]) (Fig. 5A).

4-cell to 8-cell formation

On the animal surface, ridges radiated from the animal surface uniformly over all 4 cells. Then, during 8-cell formation, a series of ridge architecture appeared where each of the prospective micromeres are forming (Fig. 2A). At the end of this stage the micromere quartet makes the typical spiralian dextral rotation to lie in the furrows between the macromeres (Conklin, 1897). The observed series of ridge architecture orientation correlated with this dextral rotation.

12-cell to 16-cell

As each apical and turret ($1q^2$) cell was being formed from the 1q cell, the surface architecture formed a characteristic dextral swirl (e.g. arrowed on Fig. 2B). This swirl reached into the developing $1q^2$ cell. As the 1q1 cell divided from the 1q cell, the surface architecture initially still spanned the two cells, but later became constricted (Fig. 2C).

The characteristic surface architecture described earlier (Tyler *et al.*, 1998) was now evident, comprising ridges radiating in all directions from the animal pole; and linear arrays swirling outwards from the turret ($1q^2$) cells and then in a dextral direction on to the macromeres.

Later cleavage stages

The surface architecture observed in the animal region was still evident at the 24-cell stage and much later cleavage stages (Fig. 2D), in which both the radiation of architecture outward from the animal pole and the continuity of pattern between cells persisted.

Microtubule network

Anti-α tubulin antibody staining revealed the location and orientation of spindles. At the 4-cell stage just prior to the formation of the 1st micromere quartet, the spindles were orientated radially outwards from the animal pole, but also displayed a dextral spiral arrangement, characteristic to this stage (Fig. 3A and File S2 in "Supplementary Material" link at:http://www.intjdevbiol.com/web/paper.php?doi=052007st). At higher magnification, astral and spindle microtubules were seen to radiate outwards from the animal pole region during the formation of the 1st micromere quartet (Fig. 3B).

The microtubular network was connected between cells via the mid body (Figs. 3C and 3D).

During the formation of the second quartet of micromeres, the spindles were again found to radiate outwards from the animal pole region and the spindle fibres spanned the 1q cell as it divided into its $1q^1$ and $1q^2$ cells (Fig. 4A), reminiscent of the orientation of surface architecture ridges observed at this stage on the same cells (as in Fig. 2C). Later cleavage stages showed some synchronisation of mitotic activity and a pervasive microtubular network (Fig. 4B).

Double labelling of both surface architecture and the microtubule network revealed a very close association between the two, such as in the centres of radius (Figs. 5A-D). This is further substantiated by examining successive optical sections of Z-series (see Files S1, S3 and S4 in "Supplementary Material" link) in which the microtubule asters seem to be continuous with the surface architecture pattern.

Moreover, the spindle-astral network exhibits a spiral patterning behaviour which with double labelling correlates with that observed in the surface architecture pattern (Figs. 6A-D). Observation of the Z-series (See "Supplementary Material" link) reveals further characteristics. Firstly, it not only indicates the three-dimensional nature of the microtubule network but the degree to which it is inter-connected throughout the whole embryo (File S4). Secondly, by manually advancing and reversing the movie clip in File S4, the spindle-astral network (such as those of the macromeres) and intercellular mid bodies give the appearance of an orientation and position that is co-ordinated together as a whole. With reference to opposite and adjacent cell counterparts and in relation to the animal-vegetal pole, the

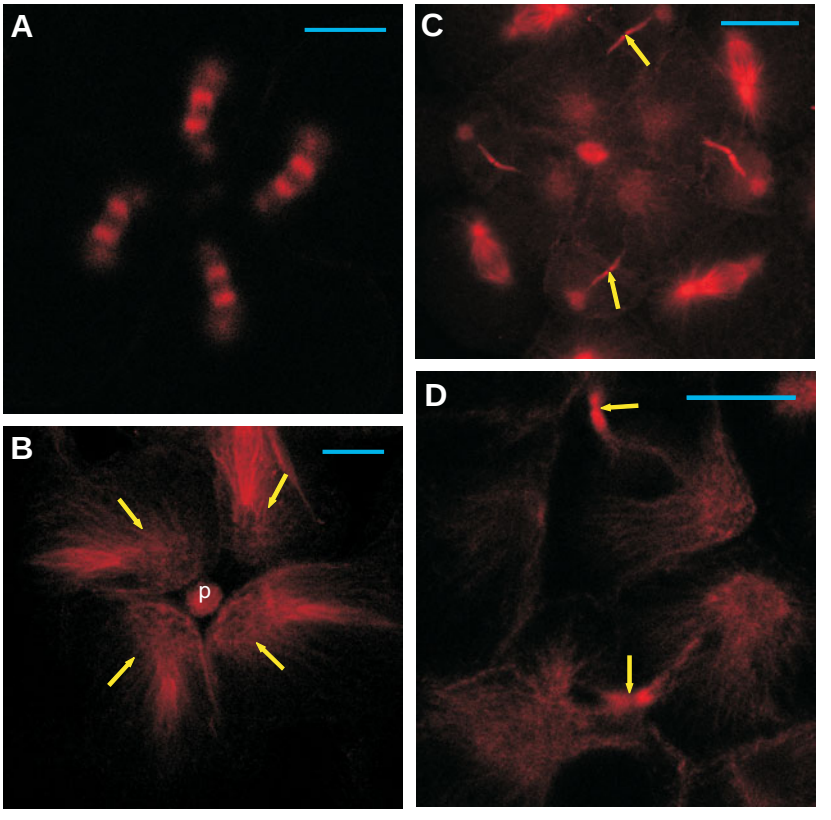

Fig. 3. Microtubule topography, revealed by FITC-anti-α tubulin antibody labelling. **(A)** *4-cell stage showing dextral curve of spindles.* **(B)** *8-cell formation, showing microtubules (arrowed) radiating from the animal pole region of the developing 1st micromere quartet.* **(C,D)** *Microtubules connected via mid-body (arrowed) at 12-cell stage (C) and 16-cell (D) stages. Scale bars A,C, 50 μm; B,D, 25 μm. p, polar body, denoting animal pole.*

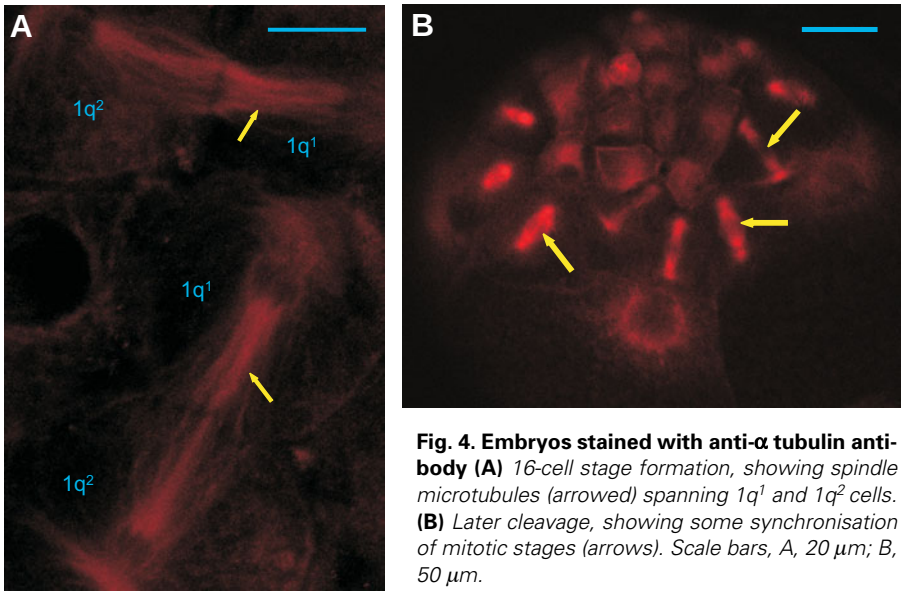

Fig. 4. Embryos stained with anti-α tubulin antibody (A) *16-cell stage formation, showing spindle microtubules (arrowed) spanning 1q¹ and 1q² cells.* **(B)** *Later cleavage, showing some synchronisation of mitotic stages (arrows). Scale bars, A, 20 μm; B, 50 μm.*

network seems to be highly orchestrated together.

Magnetic field exposure

Exposure of uncleaved embryos to a 220mT magnetic field resulted in delayed cell division and embryos in which morphology was evident with FITC-anti-α -tubulin antibody exhibited aberrant, multipolar spindles (Figs. 7A, 7B, and File S5 in "Supplementary Material" link). Embryos developed to no further than the 2-cell stage. Control embryos showed no such abnormalities and developed to normal 4-cell stages (Fig. 7D). With longer field exposure (up to 24 hours) embryos also developed abnormal macromere numbers and position.

The incompatibility of fixations for lectin and microtubule staining made double –labelling in most instances problematic for the observation of surface architecture-microtubule association. The best solution found was to focus on the fluorescent-stained microtubules at increasingly superficial levels of optical section plane, until they were indistinguishable from surface architecture topography. This may not be such a compromise: such locations represent where the microtubules are in the closest, most intimate association with the surface architecture. In such section planes, this surface-associated microtubule network exhibited swirls between the multipolar spindles (Fig. 7C). Two experiments gave a similar result. In a third experiment, the embryos developed normally (see Table).

Discussion

Dynamic changes in surface architecture

The results indicate firstly that as cleavage progresses, the surface architecture is stabilised once formed and increases in complexity. The stabilised features include the characteristic series of parallel ridges radiating outwards from the animal pole, across not only the first micromere quartets but over cells progressively more distal to the animal pole at later cleavage stages. Moreover, there is a remarkable continuation of pattern between such cells. There are also transient features, including the surface architecture swirls at the 2-cell stage and during the formation of the 1q cells leading to the 8-cell stage. From established data on cleavage activity in *Crepidula* (e.g. Conklin, 1897), it appears that the stability is thus broken by cells undergoing mitotic activity and this activity correlates with an increase in surface architecture complexity.

Surface architecture-microtubule network association

Secondly, the cytological basis of the above correlation is at least partly explained by the observed close association of the surface architecture with the underlying microtubule network and the dynamic relationship between the two. For example, association is apparent between the surface CRs and the underlying astral fibres where the latter come to a cortical focus at what could be cortical attachment points. Cortical attachment sites are well documented, for instance in the attachment of centrosomal microtubules in *Caenorhabditis* eggs (Hyman, 1989).

Our results show that this association was evident too in the orientation and developmental stages of the mitotic spindles. Thus the dextral spiralling of the mitotic spindles prior to the formation of the 1st micromere quartet correlated with the dextral spiral swirling of surface architecture seen at this stage. This spiral activity of microtubules in early molluscan cleavage has been similarly documented in the unequally cleaving embryo of the bivalve mussel *Dreissena polymorpha*, in which the spiral character is attributed to an assymetrical tilt of the D cell vegetal aster (Luetjens and Dorresteijn, 1998).

The orientation and distribution of spindle fibres throughout the 1q cell as it divided into the 1q¹ cell and 1q² cell correlated with the orientation and distribution of surface ridges radiating from the animal pole in these cells. Moreover, the point at which such architecture becomes laterally constricted correlates with the location and appearance of intercellular microtubular contacts at sites of cytokinesis. Such contacts have been observed in *Ilyanassa* eggs by Conrad *et al.*, (1994), who suggested that they stabilised the bridge constriction until the completion of cytokinesis. Moreover, if intercellular cytoplasmic continuity could be demonstrated, these bridges might well be involved in intercellular trafficking of developmentally important signalling molecules actively transported by kinesin motors along the microtubules (reviewed by Schnapp, 2003).

TABLE 1

EFFECT OF APPLIED MAGNETIC FIELD ON UNCLEAVED EGGS

Experiment	Delayed/abnormal cell division	Normal cell division	Incidence of multipolar spindles when detectable	Normal, bipolar spindles when detectable
1. + field	60	0	44 (100 %)	0
- field	0	75	0 (0 %0	58 (100 %)
2. + field	78	2	52 (96 %)	2 (4 %)
- field	0	84	0 (0 %)	67
3. + field	0	120	0 (0 %)	88
- field	0	83	0 (0%)	56

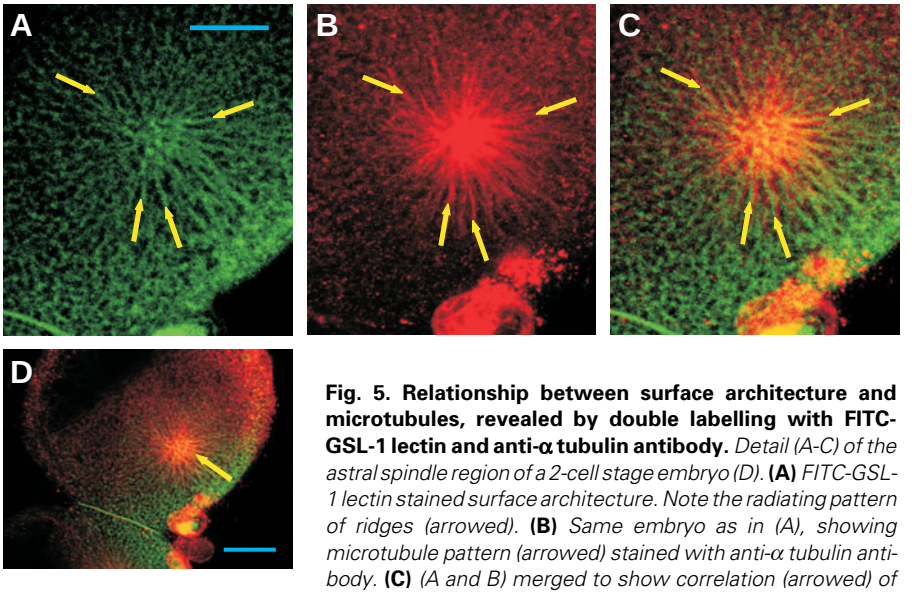

Fig. 5. Relationship between surface architecture and microtubules, revealed by double labelling with FITC-GSL-1 lectin and anti-α tubulin antibody. *Detail (A-C) of the astral spindle region of a 2-cell stage embryo (D).* **(A)** *FITC-GSL-1 lectin stained surface architecture. Note the radiating pattern of ridges (arrowed).* **(B)** *Same embryo as in (A), showing microtubule pattern (arrowed) stained with anti-α tubulin antibody.* **(C)** *(A and B) merged to show correlation (arrowed) of surface architecture and microtubule pattern.* **(D)** *Double labelling of astral spindle region (arrowed) of 2-cell stage detailed in (C). Scale bars A-C, 25 μm; D, 50 μm.*

In the induction of multipolar spindles by magnetic field exposure, surface-associating microtubules were seen to swirl between such spindles. This may indicate a perturbation of the topographical pattern of the surface architecture-microtubular association by the applied magnetic field. Normal embryos were observed after magnetic field exposure in one experiment. One possibility is that the applied field effects are cell cycle-specific.

These results indicate magnetic field specific effects. Many of these influence charged molecules associated with membranes (reviewed by Barnes, 1992). These effects include the exertion of force on moving charge carriers; alteration of the trans-membrane diffusion rate; distortion of bond angles which in turn affects protein binding and macromolecular synthesis; and change in the rate of proton tunnelling between DNA nucleotide bases (Barnothy, 1969). EMFs interact with chromatin and gene expression (Chiabrera *et al.*, 1985), so an applied magnetic field may perturb gene expression.

Morphogenetic field parameters

Thirdly, the microtubular network associated with the surface architecture is seen, particularly in the a-v presentations, to be interconnected and spatially co-ordinated throughout the embryo. Thus for example the spindle-astral networks of the macromere quartet and intercellular bridges are orientated with reference to one another and to the animal-vegetal pole, as a system moving dynamically as a whole, almost as if it were a single unit unimpeded by cell boundaries. We have suggested that the surface architecture pattern is a morphological marker for a morphogenetic field which organises cleavage (Tyler *et al.*, 1998). This close association surface architecture and microtubule network association may be explained by either one being causal upon the other, or that they have a common causality residing in a morphogenetic field. The hint of more subtle patterning which was difficult to resolve due to the limitations of the microscopy system, may reflect an underlying greater subtlety and complexity of field parameters than has been hitherto appreciated.

One hypothesis can be proposed that the surface architecture pattern is generated by tensile stresses at cortical attachment points and any other cortical attachment zones, which in turn reflect the activity of the mitotic spindle microtubular network. However, the generative basis of the latter remains unknown. An alternative hypothesis is that the peripheral or cytoplasmic microtubules may be influenced by a morphogenetic field system. If this field resides in the cortex and/or surface, the surface architecture may be the source or product of that field, which is perturbable by the magnetic field exposure. The disruption could in turn lead to the generation of multipolar spindles, perhaps by disruption of the centrosome spreading and replication cycle. This has been implicated in frog eggs exposed to a strong magnetic field, leading to mitotic apparatus reorientation (Valles, 2002). These hypotheses provide a framework for our prospective experimental focus, especially the further dissection of the surface-microtubular association and its fine – scale resolution. The developmental dynamics of the architecture in the polar lobe and lobe-forming region also deserve further interest.

Abnormal multipolar spindles have been induced by a number of agents, including colcemid, X-rays, docetaxal, cytomegalovirus, fungicides such as methyl 2-benzimidazole-carbamate and

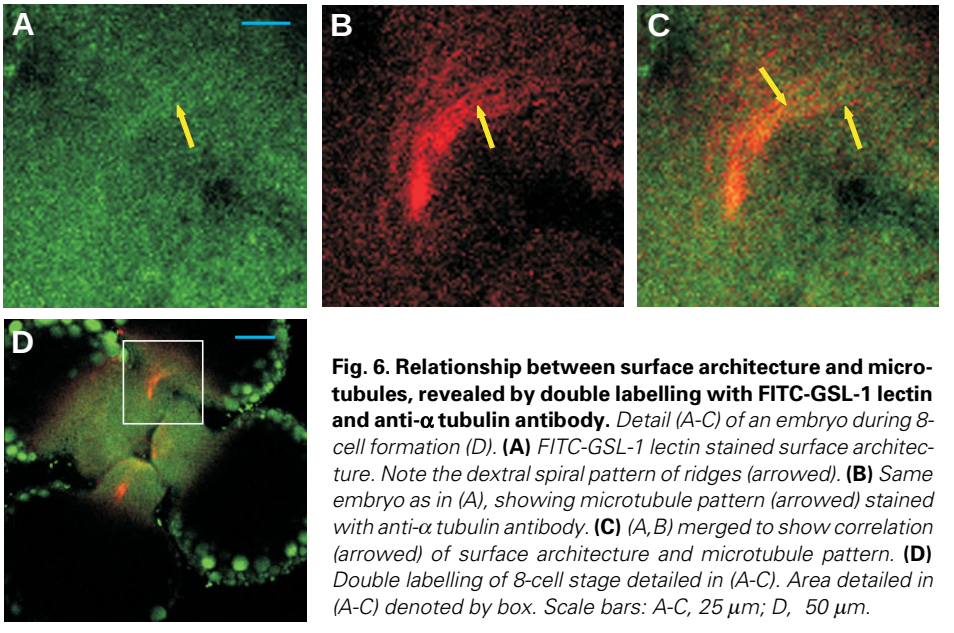

Fig. 6. Relationship between surface architecture and microtubules, revealed by double labelling with FITC-GSL-1 lectin and anti-α tubulin antibody. *Detail (A-C) of an embryo during 8-cell formation (D).* **(A)** *FITC-GSL-1 lectin stained surface architecture. Note the dextral spiral pattern of ridges (arrowed).* **(B)** *Same embryo as in (A), showing microtubule pattern (arrowed) stained with anti-α tubulin antibody.* **(C)** *(A,B) merged to show correlation (arrowed) of surface architecture and microtubule pattern.* **(D)** *Double labelling of 8-cell stage detailed in (A-C). Area detailed in (A-C) denoted by box. Scale bars: A-C, 25 μm; D, 50 μm.*

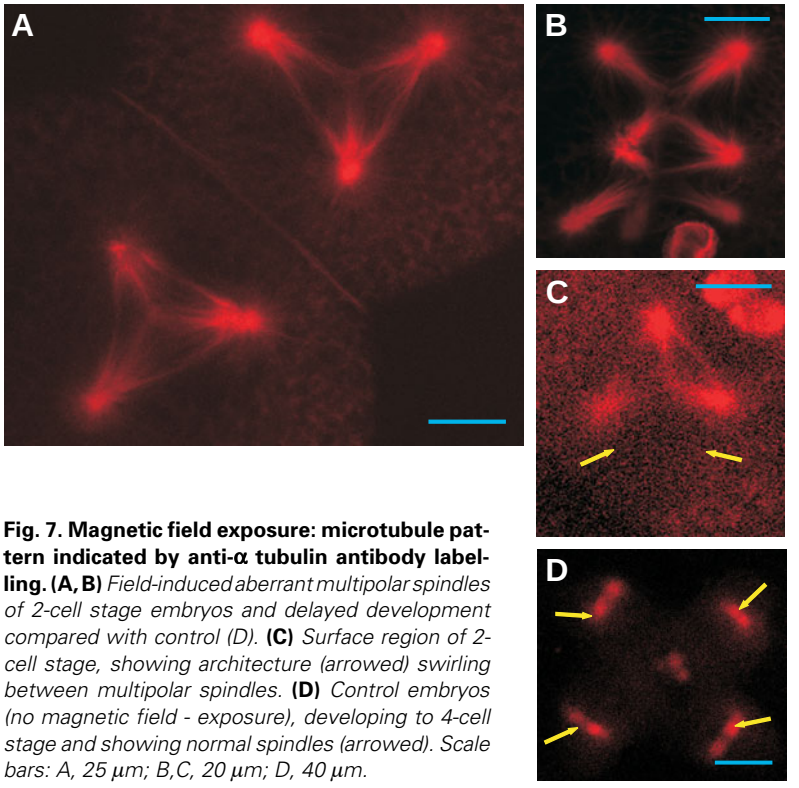

Fig. 7. Magnetic field exposure: microtubule pattern indicated by anti-α tubulin antibody labelling. (A, B) *Field-induced aberrant multipolar spindles of 2-cell stage embryos and delayed development compared with control (D).* **(C)** *Surface region of 2-cell stage, showing architecture (arrowed) swirling between multipolar spindles.* **(D)** *Control embryos (no magnetic field - exposure), developing to 4-cell stage and showing normal spindles (arrowed). Scale bars: A, 25 μm; B,C, 20 μm; D, 40 μm.*

dimethylarsinic acid (reviewed in Ochi, 2002). In the Ochi study, the intrinsic changes in the centrosomal MTOCs resulting in the multiple foci of MTOCs inherent to the multipolar spindles remain unclear, except that they are kinesin-dependent. Kinesin motor proteins provide directional cues in anchoring microtubules to the cell cortex (Yeh *et al.*, 2000). Moreover, the cytoplasmic microtubule - cell cortex interaction is a complex one: in budding yeast cells microtubules interact with a broad region of both bud and mother cell cortex, but have only a single focus in unbudded cells (Carminati and Stearns, 1997).

Endogenous fields have the potential of being carriers of morphogenetic information, rather than having only a mechanical influence (reviewed by Levin, 2002). In planarians, for example, a head-tail dipole exists, which persists in cut regenerating segments and induced field reversal led to polarity reversal in the fragments. Anode-orientated fragments developed head structure in the tail end, or two heads, or underwent polarity reversal, according to applied current density (Marsh and Beams, 1957). In earthworm segment regeneration, each segment has a specific electric potential. Segments are added until the total endogenous field potential is that of a normal full-sized worm (Kurtz and Schrank, 1955). Following vertebrate limb amputation, an injury current provides spatial cues for cells migrating into the limb and applied electrical fields have resulted in at least part limb regeneration in normally non-regenerating animals such as mammals (Becker and Sparado, 1972). Such biological effects are due to informational interactions, involving the transmission, coding and storage of information (Presman, 1970). Importantly, field theory can be applied to give a rational explanation for a wide range of human birth defects (Martinez-Frias *et al.*, 1998), but the molecular nature of which remain unknown.

In relation to this it is crucial to identify the downstream targets of endogenous fields (Levin 2002), which both detect the fields and transduce them to gene expression and cellular events. The surface architecture and the correlative pattern of the underlying microtubular network point to being end points of such targets. They both demonstrate a geometrical organisation with reference to the a-v axis and associated endogenous fields reflected by, for instance, ionic current characteristics in the molluscan embryo (Zivkovic *et al.*, 1990; Creton *et al.*, 1993). The surface-microtubular architecture patterns may be involved in the physical mediation for the co-ordination of cytokinesis, cleavage and development in relation to the primary body axis. The further study of these patterns may therefore provide crucial clues to the understanding of morphogenetic fields and their mode of action.

Materials and Methods

Crepidula fornicata

Specimens were obtained from the Spring low tide water mark (MLWS) at Hillhead, 4 miles (6.4 km) West of Portsmouth, UK (Ordnance Survey OS540 020), where they are abundant. Adults obtained from the low tide site are in preference to either the high tide location or by dredging. The force of the tide at the high water mark or the dredging process often dislodge the small male adults residing on the top of the clump of females. The males are of course essential for fertilisation of the eggs. Collected specimens were kept in aerated seawater with a coral sand - based undergravel filtration system and cooled to about 8°C to prevent egg laying. Other details of animal husbandry and egg collection are as in Tyler *et al.* (1998). Briefly, induction of egg laying involved placing clumps of animals in a separate aquarium tank, in which the temperature was raised to 12°C for 1-2 days.

Fluorescent lectin and staining

Lectin staining and confocal imaging microscopy were similar to the description in Tyler *et al.*, (1998). As far as possible, live embryos were employed for observation of surface architecture. Essentially, embryos of *Crepidula* were incubated in 100 μl/ml FITC-conjugated *Griffonia simplicifolia* lectin (GSL-1) (Vector labs) in micropore-filtered seawater containing 1 % bovine serum albumen [BFSW] for 1 h, then rinsed in BFSW. Sodium azide was omitted from the medium so as to not prevent normal development. Capping of lectin label was not observed. Where fixation was necessary, prior to lectin staining embryos were fixed in freshly prepared 4 % paraformaldehyde in Conrad's PBS (Conrad *et al.*, 1973) containing 1 % BSA, pH 7.2 [CPBS] for 30 min., then rinsed in CPBS. To remove excess paraformaldehyde, embryos were quenched in 1 mg/ml freshly prepared sodium borohydride. Lectin staining was as above, but replacing the seawater medium with CPBS.

Magnetic field exposure

Embryos in MPFSW were placed in a 3.5 cm diameter Petri dish with lid. This was placed horizontally between two bar magnets which were kept apart by perspex spacers. The centre of gravity of the embryos is nearer to the vegetal pole and so the embryos in general settle with their a-v axis parallel to the gravitational field vector. The magnetic field vector thus passed between the bar magnets in parallel to the animal-vegetal axis of the embryos. Using a gaussmeter, the magnetic field strength was measured to be 220 mT. In preliminary experiments with magnets of weaker field strength than this, embryo development was normal. Embryos were exposed to the field overnight for 12 to 16 h. They were then fixed briefly in 4 % paraformaldehyde in PHEM buffer (modified from

Schliwa and Blerkom, 1981, with the addition of 250 mM sucrose, pH 6.9) before removal from the magnetic field. Fixation was then continued in methanol at -20ºC for 30 min., then embryos were rehydrated gradually to PHEM buffer. Control embryos were incubated in the same way but omitting exposure to the magnetic field. The level of background electromagnetic radiation (<0.1 mT) was insignificant.

Microtubule staining

Embryos fixed in methanol and rehydrated as described above were incubated in 5% normal rabbit serum in CPBS [NR-CPBS] for 1 h., then overnight in YOL1/34 anti-α-tubulin antibody (Harlan seralabs) diluted to 1 in 200 in 1 % NR-CPBS. Embryos were washed in CPBS for 3 h., then incubated in either FITC- or rhodamine-conjugated anti-rat antibody diluted to 1 in 80 (Sigma) in 1% NR-CPBS for 30 min. and finally rinsed in 1 % NR-CPBS for 3 h.

Microscopy

Confocal imaging was with a Biorad MRC 600 confocal scanhead, with a krypto-argon laser emitting 2 lines at 388 nm and 514 nm. The filters were calibrated to image the FITC and rhodamine with both laser lines. Optical lenses used included an Olympus 10 x 0.3NA, a Nikon 60 x 1.4 and a Zeiss 100 x 1.3 oil objectives. Images were stored as Bio-rad's own Pic format. Single images and Z-series of optical sections, using usually a kalman filter (average of 3) were collected, at either 2 μm or 5 μm intervals, from which projections were made. Confocal imaging observations were also made using a Biorad MRC 1024 scanhead with a Nikon TE300 x 60 oil objective, but a consistently better resolution of surface architecture and microtubule networks was obtained with the MRC 600 system. Images were processed in Adobe photoshop 7 to optimise contrast and brightness.

Acknowledgements

For helpful advice we thank Colin McCaig. We are grateful for the loan of equipment from Malcolm MacCausland, David Bunberry and Barry Gleave. Tony Wade and Robert Fernandez gave technical support with confocal imaging, Ian Miller with image processing and Nina James proof-read the manuscript.

Electronic Supplementary Material for this paper, consisting of a confocal imaging Z-series (optical sections of 5 μm interval) of microtubules stained with FITC coupled anti-α tubulin antibody, is available following the "Supplementary Material" link at: http://www.intjdevbiol.com/web/paper.php?doi=052007st

Supplementary Movie 1. 2 cell stage. Association of microtubule network with surface region. 58 sections.
Supplementary Movie 2. 8-cell formation. Radiation of spindle and astral microtubules out from animal pole region. 37 sections.
Supplementary Movie 3. 16-cell stage formation. Spindle microtubules (spanning 1q1 and 1q2 cells) associating with surface region. 50 sections.
Supplementary Movie 4. 16-cell stage leading to 20-cell formation. Interconnection of microtubular network throughout the embryo. 72 sections.
Supplementary Movie 5. Field-induced aberrant multipolar spindles of 2-cell stage embryos. 46 sections.

References

BARNES, M.F. (1992). Some engineering models for interactions of electric and magnetic fields with biological systems. *Bioelectromagnetics Suppl.* 1:67-85.

BARNOTHY, M.F., editor. (1969). *Biological effects of magnetic fields*, Vol. 2. Plenum Press, New York.

BECKER, R.O. and SPARADO, J.A. (1972). Electrical stimulation of partial limb regeneration in mammals. *Bull. N.Y. Acad. Med.* 48:627-641.

BORGENS, R.B., McGINNIS, M.E., VANABLE, J.W. Jr. and MILES, E.S. (1984). Stump currents in regenerating salamanders and newts. *J. Exp Zool.* 231: 249-256.

BORGENS, R.B. and McCAIG, C.D (1989). Endogenous currents in nerve repair, regeneration and development. In *Electric Fields in Vertebrate Repair*, Alan R. Liss, New York, pp. 77-116.

BORGENS, R.D., ROULEAU, M.F. and DELANEY, L.E. (1983). A steady efflux of ionic current predicts hind limb development in the axolotl. *J. Exp. Zool.* 228: 491-503.

BORGENS, R.B., VANABLE, J.W. Jr. and JAFFE, L.F. (1977). Bioelectricity and regeneration: large currents leave the stumps of regenerating newt limbs. *Proc. Natl. Acad. Sci.* USA: 4528-4532.

BORGENS, R.B., BLIGHT, A.R. and McGINNIS, M.E. (1987). Behavioural recovery induced by applied electric fields after spinal cord hemisection in guinea pig. *Science* 238: 366-369.

BORGENS, R.B., BLIGHT, A.R. and MCGINNIS, M.E. (1990). Functional recovery after spinal cord hemisection in guinea pigs: the effect of applied electric fields. *J. Comp. Neurol.* 296:634-653.

BORGENS, R.B., TOOMBS, J.P., BREUR, G., WIDMER, W.R., WATERS, D., HARBATH, A.M., MARCH, P. and ADAMS, L.G. (1999). An imposed oscillating electric field improves the recovery of function in neurologically complete paraplegic dogs. *J. Neurotrauma* 16: 639-657. Erratum in *J. Neurotrauma* (2000). 17 (8): 727.

CARMINATI, J.L. and STEARNS, T. (1997). Microtubules orient the mitotic spindle in yeast through dynein-dependent interactions with the cell cortex. *J. Cell Biol.* 138: 629-641.

CHIABRERA, A., GIANNETI, G., GRATTAROLA, M., PARODI, M., CARLO, P. and FINOLLO, R. (1985). The role of ions in modifying chromatin structure. *Reconstr. Surg. Traumatol.* 19: 51-62.

CHIANG, M., CRAGOE, E.J.Jr. and VANABLE J.W.Jr. (1991). Intrinsic electric fields promote epithelialization of wounds in the newt, *Notophthalmus viridescens*. *Dev. Biol.* 146:377-385.

CONKLIN, E.G. (1897). The embryology of *Crepidula*. *J. Morphol.*13: 1-226.

CONRAD, G.W., WILLIAMS, D.C., TURNER, F.R., NEWROCK, K.M. and RAFF, R.A. (1973). Microfilaments in the polar lobe constriction of fertilised eggs of *Ilyanassa obsoleta*. *J. Cell Biol.* 59, 228-233.

CONRAD, A.H., STEPHENS, A.P. and CONRAD, G.W. (1994). Effect of hexylene glycol-altered microtubule distributions on cytokinesis and polar lobe formation in fertilised eggs of *Ilyanassa obsoleta*. *J. Exp. Zool.* 269(3): 188-204.

COOPER, M.S. and KELLER, R.E. (1984). Perpendicular orientation and directional migration of amphibian neural crest cells in DC electric fields. *Proc. Natl. Acad. Sci.* USA 81: 160-164.

CRETON, R., ZIVKOVIC, D, ZWANN, G. and DOHMEN, M.R. (1993). Polar ionic currents around embryos of *Lymnaea stagnalis* during gastrulation and organogenesis. *Int. J. Dev. Biol.* 37:425-431.

DENEGRE, J.M, VALLES, J.M.Jr., LIN, K., JORDAN, W.B. and MOWRY, K.L. (1998). Cleavage planes in frog eggs are altered by strong magnetic fields. *Proc. Natl. Acad. Sci. USA* 95: 14729-14732.

DOHMEN, M.R. (1992). Cell lineage in molluscan development. *Micros. Res. Tech.* 22:75-102.

DOHMEN, M.R., VAN DER MEY, J.C.R. (1977). Local surface differentiations at the vegetal pole of the eggs of *Nassarius reticulata*, *Buccinum undatum* and *Crepidula fornicata* (*Gastropoda, Prosobranchia*). *Dev. Biol.* 61:104-113

DREISCH, H. (1891). Entwicklungsmechanische Studien I-II. *Z. Wiss. Zool.* 53:160-182.

ELTINGE, E.M., CRAGOE, E.J.Jr. and VANABLE, J.W. Jr. (1986). Effects of amiloride analogues on adult *Notophthalmus viridescens* limb stump currents. *J. Comp. Biochem. Physiol.* 84: 39-44.

GOODWIN, B.C. (1984). A relational or field theory of reproduction and its evolutionary implications. In *Beyond Neo-Darwinism* (Eds. M-W. Ho and P.T. Saunders), Academic Press, London, pp 234-241.

GOODWIN, B.C. (1985). The causes of morphogenesis. *Bioessays* 3:32-36.

GOODWIN, B.C. and TRAINOR, L.E.H. (1985). Tip and whorl morphogenesis in *Acetabularia* by calcium-regulated strain fields. *J. Theor. Biol.* 117:79-105.

HINKLE, L., McCAIG, C.D. and ROBINSON, K.R. (1981). The direction of growth

of differentiating neurones and myoblasts from frog embryos in an applied electric field. *Am. J. Physiol.* 314: 121-135.

HO, M.-W., STONE, T.A., JERMAN, I, BOLTON, J., BOLTON, H., GOODWIN, B.C., SAUNDERS, P.T. and ROBERTSON, F. (1992). Brief exposure to weak static magnetic fields during early embryogenesis cause cuticular pattern abnormalities in *Drosophila* larvae. *Phys. Med. Biol*. 37: 1171-1179.

HOTARY, K.B. and ROBINSON, K.R. (1990). Endogenous electric currents and the resultant voltage gradients in the chick embryo. *Dev. Biol*. 140: 149-160.

HYMAN, A.A. (1989). Centrosome movement in the early divisions of *Caenorhabditis elegans*: a cortical site determining centrosome position. *J. Cell Biol*. 109: 1185-1193.

JAFFE, L.F. and VANABLE, J.W.Jr., (1985). Electrical fields and wound healing. In: *Clinics and dermatology*. Ed. W.H. Eaglstein. Lippincott, Philadelphia.

JAFFE, L.F., WEINSENSEEL, M.H. and SPEKSNIJDER, J.E. (1987). Injected calcium buffers block fucoid egg development. *Biol. Bull*. 173:425.

JUTILAINEN, J., HARRI, M., SAALI, K. and LAHTINEN, T. (1986). Effects of 100 Hz magnetic fields with various waveforms on the development of chick embryos. *Radiat. Environ. Biophys*. 25: 65-74.

KOCH, W.E., KOCH, B.A., MARTIN, A.H. and MOSES, G.C. (1993). Examination of the development of chicken embryos following exposure to magnetic fields. *Comp. Biochem. Physiol*. 105A(4): 617-624.

KURTZ, I. and SHRANK, A.R. (1955). Bioelectrical properties of intact and regenerating earthworms *Eisenia foetida*. *Physiol. Zool*. 28: 322-330.

LEVIN, M. (2002). Bioelectromagnetics in morphogenesis. *Bioelectromagnetics* 24:295-315.

LEVIN, M. and ERNST, S.G. (1997). DC magnetic field effects on early sea urchin development. *Bioelectromagnetics* 18(3): 255-263.

LUETJENS, C.M. and DORRESTEIJN A.W.C. (1998). Dynamic changes of the microtubule system corresponding to the unequal and spiral cleavage modes in the embryo of the zebra mussel, *Dreissena polymorpha* (*Mollusca, Bivalvia*). *Zygote* 6:239-248.

MARSH, G. and BEAMS, H.W. (1957). Electrical control of morphogenesis in regenerating *Dugesia tigrina*. *J. Cell Comp. Physiol*. 39: 191-211.

MARTINEZ-FRIAS M.L. FRIAS, J.L. and OPITZ, J. M. (1998). Errors of morphogenesis and developmental field theory. *Am. J. Med. Genet*. 76(4):291-296.

McCAIG, C.D. (1987). Spinal neurite reabsorption and regrowth depend on the polarity of an applied electric field. *Development Suppl*. 100: 31-41.

METCALF, M.E.M., SHI, R. and BORGENS, R.B. (1994). Endogenous ionic currents and voltages in amphibian embryos. *J. Exp. Zool*. 268: 307-322.

NUCCITELLI, R. (1978). Ooplasmic segregation and secretion in the *Pelvetia* egg is accompanied by a membrane-generated electrical current. *Dev. Biol*. 62: 13-33.

NUCCITELLI, R. (1988). Ion currents in morphogenesis. *Experientia* 44: 657-666.

NUCCITELLI, R. (2003). A role for endogenous electric fields in wound healing. *Curr. Top. Dev. Biol*. 58:1-26.

NUCCITELLI, R. and WILEY, L.M. (1985). Polarity of isolated blastomeres from mouse morulae: detection of transcellular ion currents. *Dev. Biol*. 109: 452-463.

OCHI, T. (2002). Role of mitotic motors, dynein and kinesin, in the induction of abnormal centrosome integrity and multipolar spindles in cultured V79 cells exposed to dimethylarsinic acid. *Mut. Res*. 499: 73-84.

PARMALEE, J.T., ROBINSON, K.R. and PATTERSON, J.W. (1985). Effects of calcium on the steady outward currents at the equator of the rat lens. *Invest. Opthalmol. Vis. Sci*. 26: 1343-1348.

PRESMAN, A.S. (1970). Electromagnetic fields and life. Plenum Press, N.Y.

ROBINSON, K.R. (1983) Endogenous electrical current leaves the limb and prelimb region of the *Xenopus* embryo. *Dev. Biol*. 97: 203-211.

SCHLIWA, M. and VAN BLERKOM, J. (1981) Structural interactions of cytoskeletal components. *J. Cell Biol*. 90: 222-235.

SCHNAPP, B.J. (2003). Trafficking of signalling modules by kinesis motors. *J. Cell Science* 116: 2125-2135.

SHI, R. and BORGENS, R.D. (1995). Three dimensional gradients of voltage during development of the nervous system as invivible co-ordinates for the establishment of embryonic pattern. *Dev. Dyn*. 202: 101-114.

STUMP, R.T. and ROBINSON, K.R. (1983) *Xenopus* neural crest cell migration in an applied electrical field. *J. Cell Biol*. 97: 1226-1233.

TYLER, S.E.B., BUTLER, R.D. and KIMBER, S.J. (1998). Morphological evidence for a morphogenetic field in gastropod mollusc eggs. *Int. J. Dev.Biol*. 42: 79-85.

UBADA, A., LEAL, J., TRILLO, M.A., JIMENEZ, M.A. and DELGADO, J.M.R. (1985) Pulse shape of magnetic fields influences chick embryogenesis. *Am. J. Anat*. 137(3): 195-536.

VALLES, J.M. (2002). Model of magnetic field-induced mitotic apparatus reorientation in frog eggs. *Biophysical J*. 82: 1260-1265.

WOODRUFF, R.I. and TELFER, W.H. (1973). Polarised intercellular bridges in ovarian follicles of the *Cecropia* moth. *J. Cell Biol*. 58: 172-188.

WOODRUFF, R.I. and TELFER, W.H. (1980). Electrophoresis of proteins in intercellular bridges. *Nature* 286: 84-86.

YEH, E., YANG, C., CHIN, E., MADDOX, P., SALMON, E.D., LEW, D.J. and BLOOM, K. (2000). Dynamic positioning of mitotic spindles in yeast: role of microtubule motors and cortical determinants. *Mol. Biol. Cell* 11: 3949-3961.

ZIVKIVIC, D. and DOHMEN, M.R. (1991). Changes in transcellular ionic currents associated with cytokinesis and polar lobe formation in embryos of *Bithynia tentaculata (Mollusca)*. *Development* 112:451-459.

ZIVKOVIC, D., CRETON, R., ZWAAN, G., DE BRUIJN, W.C. and DOHMEN, M.R. (1990). Polar localization of plasma membrane Ca^{2+}/Mg^{2+} ATPase correlates with the pattern of steady ionic currents in eggs of *Lymnaea stagnalis* and *Bithynia tentaculata (Mollusca)*. *Roux's Arch. Dev. Biol.* 199: 134-145.

Received: April 2005

Reviewed by Referees: August 2005

Modified by Authors and Accepted for Publication: September 2005